Journal of Alloys and Compounds 509S (2011) S662–S666

Contents lists available at ScienceDirect

Journal of Alloys and Compounds

journal homepage: www.elsevier.com/locate/jallcom

Stability enhancement by particle size reduction in AlH_3

P. Vajeeston*, P. Ravindran, H. Fjellvåg

Center for Materials Science and Nanotechnology, Department of Chemistry, University of Oslo, Box 1033 Blindern N-0315, Oslo, Norway

ARTICLE INFO

Article history:
Received 25 August 2010
Received in revised form
12 November 2010
Accepted 16 November 2010
Available online 24 November 2010

Keywords:
Hydrogen storage materials
Nano phase AlH_3
Cluster and thin films
Theoretical study
Nano phase and stability

ABSTRACT

Phase stability of nano-structures and possible low energy surfaces of AlH_3 polymorphs from thin film geometry have been investigated using all electron density-functional total energy calculations. The calculated structural data for α-, α′-, β-, and γ-AlH_3 modifications are in very good agreement with experimental values. The electronic structures based on parameterized HCTH functionals reveal that all polymorphs are insulators with calculated band-gap varying between 2.53 and 4.41 eV. From our theoretical simulation we have found that the (0 1 0) in α-, (1 0 0) in α′-, (1 0 1) in β-, and (1 0 1) in γ-AlH_3 surfaces are the most stable surface in the corresponding polymorphs. We have predicted that the critical size for the AlH_3 nano-cluster is less than 1 nm. As opposite to complex hydrides we have investigated so far, the calculated formation energy as a function of particle size reveal that the nano particles of AlH_3 are relatively stable than the corresponding decomposed phases.

1. Introduction

To efficiently use hydrogen as a fuel, a proper storage material is necessary that should satisfy two main criteria: (a) high hydrogen content; (b) reversible binding and releasing of hydrogen at moderate conditions. The last criterion will require a hydride compound that is neither too stable nor too unstable. AlH_3 (alane) has historically been used as an energetic component in rocket propellants [1] and more recently has been considered by many as a good candidate for hydrogen storage applications. AlH_3 is an unique binary hydride having at least six crystalline phases with different physical properties and at the same time store up to 10.1 wt.% of hydrogen [2]. Its gravimetric hydrogen density is two times higher than liquid hydrogen and much higher than that of most of the known metal hydrides. Thus, it is considered as a possible hydrogen storage material [3]. Freshly prepared alane was shown to decompose (not a stable compound) and release hydrogen at rates suitable for practical applications at relatively low temperatures (~100 °C) [4,5] which is a beneficial feature for the hydrogen storage material. Unlike complex hydrides, where one need to destabilize the system (also decomposition temperature) as well as enhance sorption kinetics, in alane one should enhance its kinetics to use it in practical applications. In general, lightweight metal hydrides are considered as storage media, but kinetic constraints limit their application. A promising approach to address this issue is to reduce the particle size of the metal hydride to the nanometer range, resulting in enhanced kinetics without the need of a catalyst [6,7]. For example, in MgH_2, a numerous studies have been focused on improving the problematic sorption kinetics, including mechanical ball milling [8–10] and chemical alloying [11,12]. The smallest particle sizes (20 nm) obtainable by these methods still primarily display bulk desorption characteristics [13]. However, recently McPhy energy system [14] demonstrated that nano phase of Mg hydride material with proper additives can store large quantities of hydrogen at low pressure within tens of minutes (for more details see Ref. [14]). In the present study we have investigated the possible low energy surfaces, role of particle size and the nanophase effect on stability in AlH_3 polymorphs.

2. Computational details

In the present work, the structural optimization and total energy calculations are performed using the DMol^3 package [15,16] which is based on the density functional theory (DFT) [17,18], and the Perdew–Burke–Eruzerhof (PBE) [19] exchange-correlation functional is adopted for generalized gradient approximation (GGA) correction. All electron Kohn–Sham wave functions are expanded in a double numerical basis with a polarized orbital (DNP). No pseudopotentials or effective core potentials were used. For the bulk phases the cell parameters and the atomic positions in the structures are fully relaxed to get the final optimized structures with minimum total energy. The convergence criteria of optimization are 1×10^{-6} eV, 0.002 eV/Å and 0.005 Å for energy, gradient and atomic displacement, respectively. The k-points were generated

* Corresponding author. Tel.: +47 22855613; fax: +47 22855441.
E-mail address: ponniahv@kjemi.uio.no (P. Vajeeston).

0925-8388/$ – see front matter © 2010 Elsevier B.V. All rights reserved.
doi:10.1016/j.jallcom.2010.11.110

Table 1
Optimized structural parameters (in Å) and calculated energy band-gap values (in eV) for AlH_3 polymorphs.

Phase (space group)	Cell constants (Å)	Sites: positional parameters	E_g (eV)
α-AlH_3 ($R\bar{3}c$.)	a = 4.502 (4.4493)[a] c = 11.848 (11.8037)[a]	Al(6b): 0, 0, 0 H(18e): (0.628),[a] 0, 1/4	2.53 (3.5[b])
α′-AlH_3 (β-AlF_3-type; *Cmcm*)	a = 6.563 (6.470)[c] b = 11.228 (11.117)[c] c = 6.654 (6.562)[c]	Al1(4a): 0, 1/2, 0; Al2(8d): 1/4, 1/4, 0 H1(8f): 0, 0.2139, 0.4447 (0, 0.197, 0.451)[c] H2(16h): 0.3094, 0.1024, 0.0505 (0.312, 0.100, 0.047)[c] H3(4c): 0, 0.4571, 1/4 (0, 0.4561, 1/4)[c] H4(8g): 0.2068, 0.2860, 1/4 (0.298, 0.277, 1/4)[c]	4.21
β-AlH_3 ($Fd\bar{3}m$)	a = 9.075 (9.0037)[d]	Al(16d): 1/2, 0, 0 H(48f): 0.4303(0.4301)[d], 1/8, 1/8	3.85
γ-AlH_3 (*Pnnm*, 58)	a = 5.4560 (5.3806)[e] b = 7.424 (7.3555)[e] c = 5.8075 (5.77511)[e]	Al1(2b): 0, 0, 1/2; Al2(4g): 0.7887, 0.085, 0 (0.7875, 0.0849, 0)[e] H1(2d): 0, 1/2, 1/2; H2(4g): 0.6737, 0.2998, 0(0.626, 0.278, 0)[e] H3(4g): 0.0977, 0.1383, 0(0.094, 0.130, 0)[e] H2(8h): 0.7992, 0.0834, 0.2979 (0.762, 0.078, 0.309)[e]	4.41

[a] Experimental value from Ref. [27].
[b] Theoretical value (with GW approximation) from Ref. [31].
[c] Experimental value from Ref. [23].
[d] Experimental value from Ref. [21].
[e] Experimental value from Ref. [24].

using the Monkhorst–Pack method with $14 \times 14 \times 14$, $8 \times 4 \times 8$, $10 \times 10 \times 10$, and $10 \times 6 \times 8$ ***k*** point mesh was used for α-, α′-, β-, and γ-AlH_3 structures, respectively.

For the AlH_3 polymorphs surface models we have employed the usual slab-supercell geometry where periodic boundary conditions are applied. An infinite stack of quasi-two-dimensional slabs are generated for the present study. Each slab is separated from its neighbors by a certain vacuum width. The thickness of a slab is usually expressed in terms of number of atomic layers, where a layer is defined as an integer number of AlH_3 formula units and are thus stoichiometric. The constructed slab corresponding to a given Miller face has an integer number of planes such that it is parallel to the surface and has a center of symmetry at the slab center. As a result, it can be mapped onto all parallel planes below it by applying symmetry operations such as translations, screw axes or glide planes and thus the resulting slab has no dipole moment. For the surface calculation we have used the similar convergence criteria we have used for the bulk phase. Similar to the bulk phases, we have used Monkhorst–Pack method with $14 \times 14 \times 1$, $8 \times 4 \times 8$, $10 \times 10 \times 1$, and $10 \times 6 \times 1$ ***k*** point mesh for the α-, α′-, β-, and γ-AlH_3 derived surfaces, respectively. The nano-clusters are constructed from the optimized geometry of the α-AlH_3 phase using nanostructure builder in the Materials Studio 5.0 [20] package. During the nano-clusters construction the AlH_3 stoichiometry was always maintained. It is quite common that, when we optimize the nano-particles/clusters it may be possible to converge towards the local minima instead of the global minimum. In order to ensure that the system stabilize in the global minimum, we have calculated the phonon frequencies which will give information about whether the optimized cluster is in local minima or in global minimum (i.e. if all the calculated frequencies are having positive value then we have considered that the system is reach the global minimum).

3. Results and discussion

3.1. Bulk phase

Among the considered polymorphs, the β-AlH_3 modification has the lowest total energy. The calculated positional and lattice parameters for the β-AlH_3 are found to be in good agreement (see Table 1) with recent experimental findings by Brinks et al. [21] and theoretical work by Ke et al. [22]. This phase consists of corner-sharing AlH_6 octahedra. The octahedra are almost regular with $\Theta_{H-Al-H} = 87.1 - 92.9^\circ$ and Al–H distances of 1.724 Å. The next energetically favorable phase is orthorhombic α′-AlH_3 modification (space group *Cmcm*). The calculated structural parameters for α′-AlH_3 are found to be in good agreement (see Table 1) with a recent experimental finding [23]. The α′-AlH_3 structure consists of AlH_6 octahedra where all hydrogen atoms are shared between two octahedra. This corner-sharing network is more open than in α-AlH_3, giving rise to hexagonal shaped pores with a diameter of ca 3.6 Å. As a result, the volume per AlH_3 unit at equilibrium is increased from ca. 33.5 $Å^3$ in α-AlH_3 to 39.3 $Å^3$ in α′-AlH_3. The calculated average Al–H distance is 1.736 Å and the Θ_{H-Al-H} varies from 87.5 to 92.5°. Yartys et al. [24] solved the structure of γ modification and found that it has an orthorhombic structure with the space group P_{nnm}. This γ modification is found to be 4.2 meV/f.u. higher in energy than α′-AlH_3 at equilibrium volume. This γ phase contains two different types of octahedra sharing their vertices and edges (see Fig. 1 in Ref. [25]). These octahedra are connected in such a way that they have a hydrogen-bridge bond formation which is different than those in other known polymorphs of AlH_3. The calculated Al–H bond distances within this structure varies between 1.721 and 1.763 Å, and H–Al–H angle varies between 86 and 94°. As the γ phase is higher in energy than the other polymorphs in the whole volume range, it may be experimentally stabilized by temperature. Similar to the α′ modification γ modification also has open pores. Hence, both modifications have almost similar equilibrium volumes (see Fig. 2b in Ref. [25]) and this is the reason why these phases often transform into the α modification as a function of time scale. The next energetically favorable structure is α-AlH_3 that consisting of corner-shared octahedra and building a distorted primitive Al sublattice. In this phase Al–H bond distance at the equilibrium is 1.712 Å and H–Al–H angle is almost 90°. It is interesting to note that the involved energy difference between the α-, α′-, β-, and γ-AlH_3 is very small and hence one can easily modify one polymorph into another by application of temperature or pressure. These findings are consistent with our previous investigation where we have used different computational approach and predicted several pressure induced structural transition in AlH_3 [25].

The energy difference between the involved phases: α′-, α-AlH_3 is −16 meV (−1.55 kJ/mol), β-α-AlH_3 −31 meV (−2.99 kJ/mol), γ-α-AlH_3 is −11.8 meV (−1.14 kJ/mol), and γ-, α′-AlH_3 is −4.2 meV (−0.4 kJ/mol). However, recent theoretical finding suggested that, when one include the zero-point energy correction in to the total energy, γ-AlH_3 is more stable than α-AlH_3 by 1.2 kJ/mol [26]. One

should remember that the calculated results are valid only for defect free ideal single crystal at low temperatures. However, the experimental findings show that depending upon the synthesis route/conditions one can stabilize different polymorphs of AlH_3 [21,23,24,27]. It is worth to note that, due of the compact atomic arrangement and less pore size, experimentally α modification becomes very stable compared to the other modifications.

All AlH_3 polymorphs have finite energy gaps (E_g; vary between 2.53 and 4.41 eV) between the valence band maximum (VB) and the conduction band minimum (CB) and are hence proper insulators. It is also commonly recognized that theoretically calculated energy gaps for semiconductors and insulators are strongly dependent on the approximations used and in particular on the exchange and correlation terms of the potential. In general, compared to experimental band-gap values, density-functional calculations always underestimate band-gap values significantly. In order to get better band-gap values, we have used parameterized HCTH [28] functionals for the density of states calculations in the present study. In general, HCTH functions gives better band-gap values [28]. HCTH is a semi-empirical GGA functional which includes local exchange-correlation information (for more details see hcth). For example, the calculated GGA band-gap value for the α-MgH_2 is 4.2 eV [29] which is lower than the obtained HCTH band-gap value of 4.96 eV. The corresponding experimentally reported value is 5.16 eV [30]. Hence, one can expect that the AlH_3-polymorphs might have band gap value higher than the corresponding predicted band-gap values. It should be noted that the calculated band-gap value for α-AlH_3 is lower than that from other theoretical report based on GW approximation (3.5 eV) [31]. In general, HCTH functions gives better band-gap values than than that obtained from the pure LDA and GGA.

3.2. Surface energy study

For the surface calculations the unrelaxed slabs have been cut from the optimized bulk crystal, where bulk structures have been fully relaxed with respect to stress and strain. All atoms in such created slabs have been allowed to relax using the minimization of forces acting on them. The thickness of a slab and the width of the vacuum layer can affect the calculated surface energy of the surface model. Therefore, we have first performed the effect of these variables on the surface energy to determine the converged parameters. We have performed these calculations for slab thicknesses of 3–15 layers and a variety of different vacuum widths.

The surface energy of a crystal can be calculated using the following equation

$$E_{surf}(n) = \frac{E_{tot}(n) - E_{bulk}(n)}{2A} \quad (1)$$

where E_{tot} and A are the total energy and total surface area, respectively of the slab-supercell. E_{bulk} refers to the energy of the bulk AlH_3 polymorph containing the same number of molecular units as the slab. Since the constructed supercell of slab has two surfaces, the energy difference is normalized by twice the area of each surface in Eq. (1). Fig. 1 shows the variation in the calculated surface energy as a function of layer thickness in the (0 1 0) direction for α-AlH_3. It clearly indicates that the surface energy becomes stabilized from eighth layer onwards. In all the studied thin film geometries we have found that 8–10 Å layer thickness supercell (depending upon the surface) is sufficient to get the well converged surface energy.

The calculated surface energies for all the possible low energy surfaces are given in Table 2 for the AlH_3 polymorphs. The calculated surface energies for different surfaces of α-AlH_3 are vary from 0.68 to 1.99 J/m^2 depending upon the surface. The surface energy for α-AlH_3 is almost the same for (0 1 0), (0 1 1), (1 0 0), and (1 1 1) surfaces. The possible reason is that in α-AlH_3 the (0 1 0), (0 1 1), (1 0 0), and (1 1 1) surfaces have almost a similar atomic arrangement. Similarly, in β-polymorph both (0 1 0)–(1 0 0), and (0 1 1)–(1 1 0) surfaces have almost the same surface energy. Similarly, in γ-polymorph (0 1 0) and (0 1 0) have a similar surface energy. Among the considered surfaces, the (0 1 0) in α-, (1 0 0) in α′-, (1 0 1) in β-, and (1 0 1) in γ-AlH_3 surfaces have the lowest surface energy and hence they become the most stable surface in the corresponding polymorphs. The calculated lowest surface energy for these polymorphs in AlH_3 are in the following order γ < β < α′ < α. It is interesting to note that the calculated surface energy values for these surfaces indicate that the energy cost to break Al–H bond will be similar to breaking Mg–H bonds in α-MgH_2 [32].

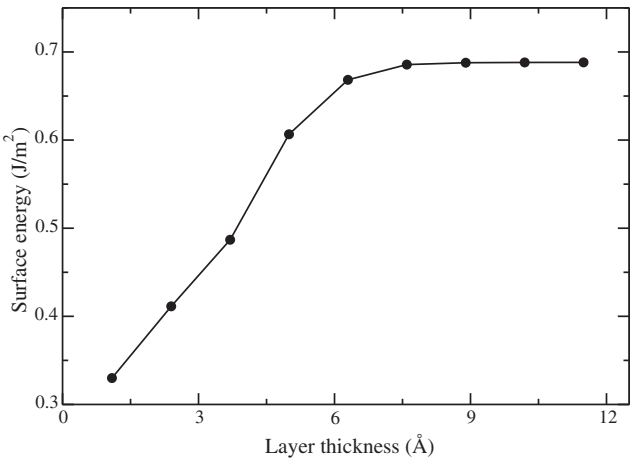

Fig. 1. Calculated surface energy as a function of layer thickness for α-AlH_3 in the thin film geometry with (0 1 0) surface.

3.3. Results from nanoparticle modelling

From the variation in the interatomic distances compared with bulk materials it should be anticipated that nano-phase materials have different physical and chemical property than the bulk materials. Once we reduce the particle size beyond certain range (called critical particle size), most of the atoms will be exposed to the surface. It is at this region where the properties of the material begins to differ drastically from that of the bulk materials. In order to identify the critical particle size we have calculated the total energy as a function of the cluster size for AlH_3 as shown in Fig. 2. From Fig. 2 it is evident that if the cluster size decreases the total energy becomes more positive. In particular there is a steep increase in the total energy when the size of the cluster is below 1 nm for α-AlH_3. Further, the reduction in the total energy for the nanoparticles suggest the changes in thermodynamical properties and in particular the hydrogen sorption temperature is expected to reduce in nanophases compared with that in bulk materials. The reason is that the surface-to-volume ratio increases upon decreasing the

Table 2
Calculated surface energy (in J m^{-2}) for AlH_3 polymorphs in different possible low-energy surfaces.

Direction	α	α′	β	γ
(0 0 1)	1.99	0.89	0.98	1.39
(0 1 0)	0.68	1.30	0.81	1.38
(0 1 1)	0.70	0.69	0.76	0.68
(1 0 0)	0.69	0.63	0.81	1.09
(1 0 1)	0.94	0.71	0.52	0.45
(1 1 0)	1.30	1.02	0.76	1.17
(1 1 1)	0.70	0.77	1.05	0.55

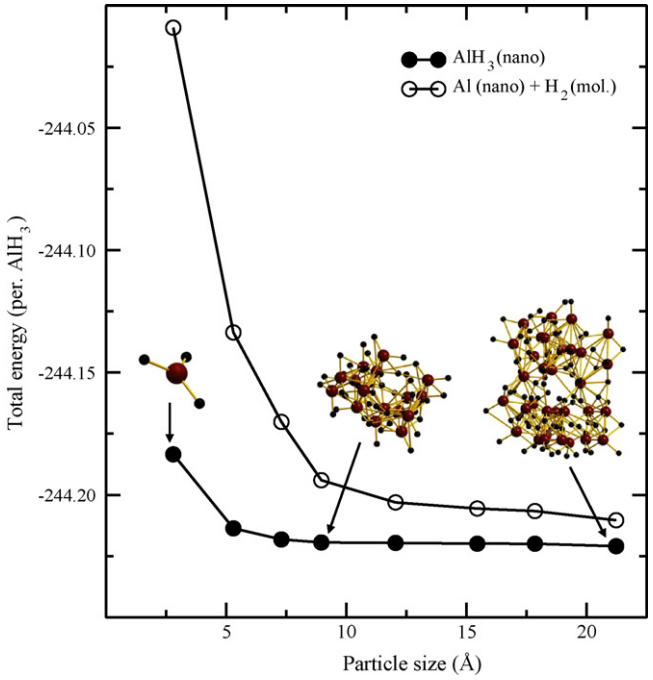

Fig. 2. Calculated total energy as a function of particle size for the AlH_3 nano-clusters (in filled circle) and nano particles of Al with the H_2 molecule [i.e. E_{Al} (nano) + $(3/2)E_{H_2}$ (mol.)] (in open circle).

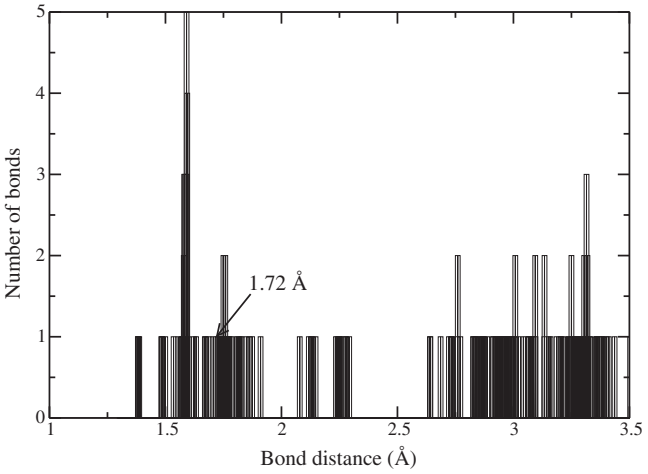

Fig. 4. Calculated interatomic distance between Al and H in an optimized nano-clusters derived from α-AlH_3. Arrow mark indicates the Al–H distance for the bulk α-AlH_3 phase.

cluster size. Since the surface atoms have lower coordination (generally found to occupy the less stable top and bridge sites) than that in bulk materials, the average number of bonds between constituents is lower for smaller clusters. This could explain why the decomposition temperature for nanoparticles are usually lower than that in bulk materials.

If one compare the variation in total energy with particle size for α-AlH_3 and that with the combination of nanoparticles of Al with H_2 molecule (see Fig. 2), even the particle size below 1 nm the nanoparticle from α-AlH_3 is energetically stable compared with the corresponding decomposed phases (i.e. nanoparticles of Al with H_2 molecule). Especially, below the critical particle size, i.e. ca. 1 nm, the total energy get more positive (i.e. highly unstable) for the combination of nanoparticles of Al with H_2 molecule. This is opposite to the conclusion we have arrived on nanoparticles of MgH_2 and borohydrides, where, below the critical particle size these nanoparticles decompose and release hydrogen. So, the present result suggest that, unlike other hydrides we have investigated for their nanophase aspects, one can stabilize nanoparticles of AlH_3 even below 1 nm size. In order to substantiate this observation we have calculated the formation energy (ΔH) as a function of particle size using the following equation.

$$\Delta H = E_{AlH_3}(\text{nano}) - \left[E_{Al}(\text{nano}) + \frac{3}{2}E_{H_2}(\text{mol.})\right] \quad (2)$$

where E_{AlH_3} (nano) and E_{Al} (nano) are the total energy of the AlH_3 and Al nano-clusters, respectively. E_{H_2} (mol.) refers to the total energy of the hydrogen molecule. The calculated ΔH value for the bulk α-AlH_3 phase is −5.99 kJ/mol. This result is in good agreement with the experimental (varies from −9.0 to −11.4 kJ/mol) [33–35] as well as other theoretical findings (−5.0 kJ/mol) [36]. In reality, due to the lower formation energy AlH_3 easily decomposes into Al and H_2 on elapse of time. It should be noted that the phase diagram study on Al–H system shows that AlH_3 is a metastable compound at ambient conditions and it become stable at high hydrogen pressure (∼7 kbar at room temperature) [37]. The calculated ΔH as a function of the particle size is displayed in Fig. 3. The critical particle size is found to be 1 nm and the corresponding ΔH value is −5.8 kJ/mol, which is similar to that in the bulk phase (i.e. the system is unstable). From Fig. 3 it is evident that when the particle size is smaller (below ∼1 nm) the formation energy of the system becomes much higher and the system can be more stable compared to Al + H_2). This clearly tell us that when the particle size is smaller and smaller the system becomes more stable. On the other hand, in MgH_2, the particle size reduction destabilize the system [32,38,39]. The possible reason for such deviation may be due to the different chemical bonding present in these two materials. In MgH_2 the interaction between the Mg and H is almost pure ionic [40] while in AlH_3 the interaction between Al and H is mixed iono-covalent bonding. These findings clearly indicate that, depending upon the system, the reduction in the particle size may either stabilize or destabilize the system. It should be noted that, when we increase the cluster size above the critical size, these nano-objects will have core AlH_3 structural units which makes them behave like a bulk system. This is one of the reason why the calculated total energy and formation energy are almost constant for above 1 nm particles and the formation energies are almost similar to that of the bulk system.

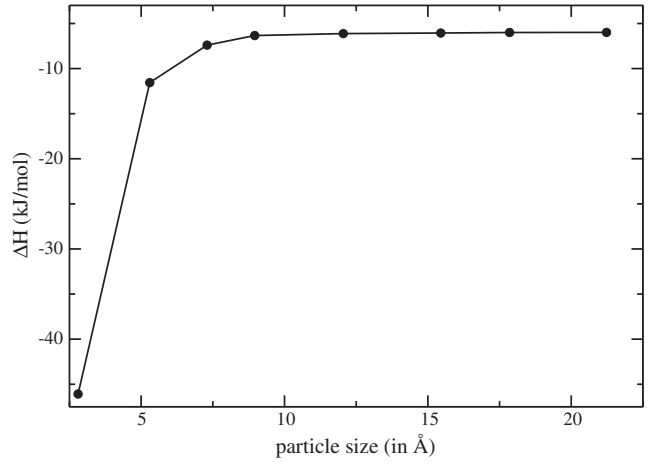

Fig. 3. Calculated formation energy as a function of particle size for the AlH_3 nano-clusters.

Though AlH_3 is one of the promising candidate for hydrogen storage application, it is not a stable compound and its property changes with time when store it in ambient condition and especially releases the hydrogen around 100 °C [4,5]. In order to increase the stability of this system one must reduce the particle size beyond the critical particle size. The present study suggest that the particle size of α-AlH_3 clusters below 1 nm might have the required physical/chemical properties for the practical applications.

The calculated Al–H distances versus number of bonds (see Fig. 4) for the critical clusters indicate that the values were scattered compared with that in the corresponding bulk phase. This type of structural arrangement is expected in nano- and amorphous-phases with no three dimensional crystallinity owing to reduction in coordination number of atoms. It is note worthy to inform here that most of the Al–H distances are reduced compared with the bulk AlH_3 systems. This enhancement in the bond strength is another indication for the stabilization of the AlH_3 nano-particles.

4. Conclusion

At ambient pressure and zero Kelvin AlH_3 stabilizes in the β polymorph. The calculated structural data for α-, α′-, β-, and γ-AlH_3 modification are in very good agreement with experimental values. The electronic structures reveal that all polymorphs are nonmetals with calculated band-gap varying between 2.53 and 4.41 eV. From supercell total energy calculation the possible low-energy surfaces and stability of nano-clusters was identified. Our theoretical simulation we have found that the (0 1 0) in α-, (1 0 0) in α′-, (1 0 1) in β-, and (1 0 1) in γ-AlH_3 surfaces has the lowest surface energy and hence they becomes the most stable surface in the corresponding polymorphs. We have predicted that the critical particle size for the AlH_3 nano-cluster is less than 1 nm. If one reduces the size below the critical size, the stability of the cluster increases drastically and we have identified that in such objects almost all atoms are exposed to the surface. The present study suggest that, in order to enhance the stability of AlH_3 as a hydrogen storage material, one must reduce the particles size below the critical size.

Acknowledgments

The authors gratefully acknowledge the Research Council of Norway (project numbers 460829 and 185309/S30) and European Union seventh frame work program under the “NanoHy” (Grant agreement no.: 210092) project for financial support. PV gratefully acknowledges the Research Council of Norway for providing the computer time at the Norwegian supercomputer facilities and V. Yartys for useful discussions.

References

[1] C. Johnson, M. Chan Evaluation of AlH3 for Propellant Application. NAWCWD TP 8524, 2002, May.
[2] F.M. Brower, N.E. Matzek, P.F. Reigler, H.W. Rinn, C.B. Roberts, D.L. Schmidt, J.A. Snover, K. Terada, J. Am. Chem. Soc. 98 (1976) 2450.
[3] L. Schlapbach, A. Züttel, Nature 414 (2001) 353.
[4] J. Graetz, J. Reilly, J. Phys. Chem. B 109 (2005) 22181.
[5] G. Alefeld, J. Völkl (Eds.), Topics in Applied Physics, vol. 29, Springer, Berlin, 1978.
[6] C.P. Baldé, B.P.C. Hereijgers, J.H. Bitter, K.P. de Jong, Angew. Chem., Int. Ed. 45 (2006) 3501.
[7] A. Gutowska, L. Li, Y. Shin, C.M. Wang, X.S. Li, J.C. Linehan, R.S. Smith, B.D. Kay, B. Schmid, W. Shaw, M. Gutowski, T. Autrey, Angew. Chem., Int. Ed. 44 (2005) 3578–3582.
[8] A. Zaluska, L. Zaluski, J.O. Ström-Olsen, J. Alloys Compd. 288 (1999) 217.
[9] A. Zaluska, L. Zaluski, J.O. Ström-Olsen, Appl. Phys. A: Mater. Sci. Process 72 (2001) 157.
[10] S. Orimo, H. Fujii, K. Ikeda, Acta Mater. 45 (1997) 331.
[11] J. Huot, G. Liang, R. Schultz, Appl. Phys. A: Mater. Sci. Process 72 (2001) 187.
[12] J. Huot, J.F. Pelletier, L.B. Lurio, M. Sutton, R. Schulz, J. Alloys Compd. 348 (2003) 319.
[13] G. Liang, J. Huot, S. Boily, A.V. Neste, R. Schulz, J. Alloys Compd. 292 (1999) 247.
[14] http://www.mcphy.com/en/news/releases-245.php.
[15] B. Delley, J. Chem. Phys. 92 (1990) 508.
[16] B. Delley, J. Chem. Phys. 113 (2000) 7756.
[17] P.C. Hohenberg, W. Kohn, Phys. Rev. B 136 (1964) 864.
[18] W. Kohn, L.J. Sham, Phys. Rev. A 140 (1965) 1133.
[19] J.P. Perdew, K. Burke, M. Ernzerhof, Phys. Rev. Lett. 77 (1996) 3865.
[20] http://accelrys.com/products/materials-studio/.
[21] H.W. Brinks, W. Langley, C.M. Jensen, J. Graetz, J.J. Reilly, B.C. Hauback, J. Alloys Compd. 433 (2006) 180.
[22] X. Ke, A. Kuwabara, I. Tanaka, Phys. Rev. B 71 (2005) 184107.
[23] H.W. Brinks, A. Istad-Lem, B.C. Hauback, J. Phys. Chem. B 110 (2006) 25833.
[24] V.A. Yartys, R.V. Denys, J.P. Maehlen, C. Frommen, M. Fichtner, B.M. Bulychev, H. Emerich, Inorg. Chem. 46 (2007) 1051.
[25] P. Vajeeston, P. Ravindran, H. Fjellvåg, Chem. Mater. 20 (2008) 5999.
[26] Y. Wang, J-A. Yan, M.Y. Chou, Phys. Rev. B 77 (2008) 014101.
[27] J.W. Turley, H.W. Rinn, Inorg. Chem. 8 (1969) 18.
[28] A.D. Boese, N.C. Handy, J. Chem. Phys. 114 (2001) 5497.
[29] P. Vajeeston, P. Ravindran, A. Kjekshus, H. Fjellvåg, Phys. Rev. Lett. 89 (2002) 175506.
[30] B. Pfrommer, C. Elsässer, M. Fähnle, Phys. Rev. B 50 (1994) 5089.
[31] M.J. van Setten, V.A. Popa, G.A. de Wijs, G. Brocks, Phys. Rev. B 75 (2007) 035204.
[32] P. Vajeeston, P. Ravindran, H. Fjellvåg, Nanotechnology 19 (2008) 275704.
[33] J. Graetz, J.J. Reilly, J. Alloys Compd. 424 (2006) 262.
[34] G.C. Sinke, L.C. Walker, F.L. Oetting, D.R. Stull, J. Chem. Phys. 47 (1967) 2759.
[35] S. Orimo, Y. Nakamori, T. Kato, C. Brown, C.M. Jensen, Appl. Phys. A 83 (2006) 5.
[36] C. Wolverton, V. Ozolins, M. Asta, Phys. Rev. B 69 (2004) 144109.
[37] J. Graetz, J. Reilly, V.A. Yartys, J.P. Maehlen, B.M. Bulychev, V.E. Antonov, B.P. Tarasov, I.E. Gabis, MH2010 contribution.
[38] P. Vajeeston, P. Ravindran, H. Fjellvåg, 2010, unpublished.
[39] R.W.P. Wagemans, J.H. van Lenthe, P.E. de Jongh, A.J. van Dillen, K.P. de Jong, J. Am. Chem. Soc. 127 (2005) 16675.
[40] P. Vajeeston, P. Ravindran, B.C. Hauback, H. Fjellvåg, A. Kjekshus, S. Furuseth, M. Hanfland, Phys. Rev. B 73 (2006) 224102.